

# Influences of graphene oxide on biofilm formation of gram-negative and gram-positive bacteria

Chao Song<sup>1</sup> · Chun-Miao Yang<sup>1</sup> · Xue-Fei Sun<sup>1</sup> · Peng-Fei Xia<sup>1</sup> · Jing Qin<sup>1</sup> · Bei-Bei Guo<sup>1</sup> · Shu-Guang Wang<sup>1</sup>

Received: 26 May 2017 / Accepted: 24 October 2017 / Published online: 15 November 2017  
© Springer-Verlag GmbH Germany 2017

**Abstract** In this study, we evaluated the influences of graphene oxide (GO) on biofilm formation. *Escherichia coli* MG1655 and *Bacillus subtilis* 168 were used as models for Gram-negative and Gram-positive bacteria. The growth profiles and viability assays indicated that GO exhibited a high antibacterial activity, of which the negative effects on bacteria growth raised with the increasing GO concentration. The antibacterial activity of GO was mainly attributed to the membrane stress and ROS-independent oxidative stress. Moreover, it was worthy to note that the biofilm formation was enhanced in the presence of GO at low dosage whereas inhibited in the high-concentration GO environment. These results could be explained by the roles of the dead cells, which were inactivated by GO. When the concentration of GO was limited, only a part of the cells would be inactivated, which may then serve as a protection barrier as well as the necessary nutrient to the remaining living cells for the formation of biofilm. In contrast, with a sufficient presence of GO, almost all cells can be inactivated completely and thus the formation of biofilm could no longer be triggered. Overall, the present work provides significant new insights on the influence of

carbon nanomaterials towards biofilm formation, which has far-reaching implications in the field of biofouling and membrane bioreactor.

**Keywords** Biofilm · Graphene oxide · Dead cell · Oxidative stress · Antibacterial mechanism

## Introduction

Graphene oxide (GO), one of the most important graphene derivatives, has attracted great attention in the scientific communities due to its remarkable physicochemical properties (Xia et al. 2015). With the rapidly increasing production and application, large quantities of GO are released into aquatic environment, including surface water and groundwater (Sotirelis and Chrysikopoulos 2015). Consequently, significant researches have been conducted on the fate, transport, and behavior of the released GO. Chowdhury et al. (2013) studied the colloidal properties and stability of GO in various synthetic and natural waters. Sotirelis and Chrysikopoulos (2015) investigated the deposition and attachment of GO nanoparticles onto quartz sand. Similar to other carbon nanomaterials, GO is toxic to human and bacterial cells (Ding et al. 2005, Manna et al. 2005). Various bacteria, such as *Pseudomonas aeruginosa*, *Escherichia coli*, and *Staphylococcus aureus*, could be inactivated by GO via membrane stress and oxidative stress (Akhavan and Ghaderi 2010, Gurunathan et al. 2012). Therefore, the released GO would be a potential threat to ecology, and it is an urgent and important subject to explore the adverse impacts of GO on aquatic ecosystems.

Responsible editor: Diane Purchase

**Electronic supplementary material** The online version of this article (<https://doi.org/10.1007/s11356-017-0616-8>) contains supplementary material, which is available to authorized users.

✉ Xue-Fei Sun  
xuefeisun@sdu.edu.cn

✉ Shu-Guang Wang  
wsg@sdu.edu.cn

<sup>1</sup> Shandong Key Laboratory of Water Pollution Control and Resource Reuse, School of Environmental Science and Engineering, Shandong University, Jinan 250100, China

Bacteria mainly exist as planktonic isolated cells or sessile communities in aquatic ecosystems, and most bacteria live attached to different surfaces by forming microbial consortia referred to as biofilm (Costerton et al. 1999, Schembri et al. 2003). In general, bacterial biomass in various environments is constituted by biofilm, a protected mode of growth, which allows survival in a hostile environment (Costerton et al. 1999). Moreover, many beneficial applications of biofilm have been reported, such as degradation of organic contaminants (Jewell et al. 2016), in situ remediation of natural water and sediment (Lv et al. 2017, Reid et al. 2016), and as biocontrol agents in certain plants (Rudrappa et al. 2008). However, there are also some negative effects of biofilm, such as sources of antibiotic-resistant bacteria (Blaustein et al. 2015), causing biofouling of pipes and membrane reactors (Bar-Zeev et al. 2015) and contaminating drinking water (Liu et al. 2016). In consideration of the ubiquity and multiple roles of biofilm in aquatic environment, it is significant to understand the possible impacts of GO on biofilm.

Although several studies have been conducted on the biotoxicity of GO, they mainly focused on the planktonic isolated bacteria (Musico et al. 2014, Perreault et al. 2015). In general, most planktonic-isolated bacteria could attach to solid surfaces to form biofilm (Costerton et al. 1999). Therefore, the released GO would first encounter planktonic cells and take part in the formation of biofilm. Moreover, bacteria in biofilm often exhibit resistance in an adverse environment (Greendyke and Byrd 2008), implying that toxic substances might have different effects on biofilm. Rodrigues and Elimelech (2010) studied the effects of single-walled carbon nanotube on bacterial growth and biofilm formation. GO is associated with different structure and properties between single-walled carbon nanotube; thus, the toxic and inactivation mechanism of GO on biofilm could be different. Nonetheless, the existing literature on environmental behavior of GO on biofilm formation remains limited.

Herein, the main objective of this work was to investigate the influence of GO on the formation of biofilm. *Escherichia coli* MG1655 and *Bacillus subtilis* 168 were selected as model bacteria of Gram-negative bacteria and Gram-positive bacteria, respectively. The growth profiles and viability assays were performed to evaluate the antibacterial activity of GO. Besides, the oxidative stress and the roles of dead cells were analyzed to explore the antibacterial mechanisms of GO. This work could provide meaningful insights on the cytotoxicity behavior of GO in natural and engineered aquatic systems.

## Materials and methods

### Preparation and characterization of GO

Graphite oxide was synthesized by the oxidation of graphite powder (50 mesh, Aladdin) following a modified Hummers

method (Hummers Jr and Offeman 1958, Sun et al. 2015). Briefly, graphite (0.5 g) and NaNO<sub>3</sub> (0.5 g) were mixed with 23 mL concentrated sulfuric acid in a 100-mL round-bottom flask at 0 °C in an ice-water bath. KMnO<sub>4</sub> (3 g) was slowly added into the suspension with constant stirring to keep the temperature under 20 °C. Then, the flask was put into a thermostat water bath and the temperature was maintained at 35 °C for 1 h. After that, deionized water (40 mL) was added, and the temperature was raised to 90 °C and held for 30 min. Subsequently, 100 mL of deionized water was added to terminate the reaction, followed by the addition of 5 mL H<sub>2</sub>O<sub>2</sub> (v/v, 30%). Finally, the suspension was centrifuged at 5000 rpm for 15 min, and the supernatant was decanted. The precipitate was washed with deionized water until the pH was neutral (~7.0) and then lyophilized to obtain GO powder. The obtained GO was re-suspended with deionized water and treated with ultrasonication for 30 min to get GO dispersions. Scanning electron microscopy (SEM) was performed to determine physical morphology of GO. The chemical structure and properties were characterized via UV, EDS, FTIR, and Raman analysis.

### Bacterial strains and culture conditions

In this study, *E. coli* MG1655 (*E. coli*, obtained from The Coli Genetic Stock Center, Yale University), and *B. subtilis* 168 (*B. subtilis*, acquired from Prof. Li Li's Lab, Shandong University) were selected as typical Gram-negative bacteria and Gram-positive bacteria, respectively. For the cultivation of both bacteria, Luria-Bertani (LB) media was used as eutrophic conditions, and minimal M63 supplemented with 0.2% (w/v) glucose was applied as oligotrophic conditions. Besides, the cultivation temperature was 37 °C for *E. coli* and 30 °C for *B. subtilis*.

### Cell growth and biofilm formation assays

The growth profiles and viability experiments of both bacteria were carried out with different dosages of GO to evaluate the antibacterial activity of GO. For growth profiles, the optical density (OD) at 600 nm was recorded at different time intervals with a UV-2000 spectrophotometer (UNICO, USA). For viability experiments, the bacterial suspensions with different concentrations of GO were incubated at 200 rpm for 2 h. After that, the suspensions were spread on agar plates and incubated for 24 h. Then, the numbers of bacteria colonies were counted to calculate the viability.

Biofilm formation assays were operated according to reported methods (Jackson et al. 2002, Radzig et al. 2013). Briefly, overnight bacteria cultures (20 µL) were inoculated 1:100 into 24-well polystyrene plates, which contained 2 mL medium solution with different concentrations of GO (0, 10, 20, 40, 80, 160 mg/L). All the plates were incubated at 90 rpm

for 48 h. Then, the plates were carefully washed by phosphate buffer saline (PBS, pH = 7.4) to remove planktonic cells. The attached cells were stained with 2 mL crystal violet (0.1%) for 15 min. After staining, the wells were washed three times with PBS. Finally, 2 mL ethanol was added, and OD<sub>600</sub> was measured to quantify the attached cells. All experiments were repeated at least in triplicate, and the error bars represent the standard deviations calculated for each independent experiment.

### Biofilm formation in the presence of dead cells

Biofilm biomass with the addition of dead cells was monitored to evaluate the role of dead cells during biofilm formation. The experiments were carried out according to the method described by Rodrigues and Elimelech (2010). Briefly, both *E. coli* and *B. subtilis* were overnight cultured in 50 mL M63 media containing 0.2% glucose (*m/v*). The cells were washed thrice with 20 mL PBS by centrifugation at 6000 rpm for 10 min and then re-suspended by adding 20 mL M63 media without glucose. Cell re-suspension (2 mL) was taken and analyzed with plate count method to quantify the number of cells. The rest of the cells were inactivated via autoclave treatment at 120 °C for 20 min, and the dilution-plate method was applied in triplicate to ensure the death of all cells. Then, the inactivated cells were diluted with M63 media to obtain different concentrations of dead cells for biofilm assay. Each dead cell dilution (2 mL) was added into wells of a 24-well plate, and the wells containing 2 mL M63 without dead cells were also performed as control. Overnight bacteria cultures (20 µL) were then inoculated in all wells, and the plate was cultivated for 48 h. The biofilm formation was measured with the same method in the “Cell growth and biofilm formation assays”. All experiments were repeated four times.

### Detection of superoxide anion (O<sub>2</sub><sup>•-</sup>)

The possibility of superoxide anion (O<sub>2</sub><sup>•-</sup>) production was assessed following the method by the reduction of XTT (2, 3-bis (2-methoxy-4-nitro-5-sulfophenyl)-2H-tetrazolium-5-carboxanilide, Sigma) (Sutherland and Learmonth 1997). XTT solution (0.4 mM) and GO dispersion (40 mg/L) were prepared with PBS. Then, XTT solution (10 mL) was mixed with GO dispersion (10 mL), and the mixture was placed in dark for 5 h. Samples were collected and filtered through 0.45-µm nylon membranes. The absorbance of filtered solutions was measured at 470 nm to detect XTT-formazan, which was generated from the reaction of O<sub>2</sub><sup>•-</sup> and XTT.

### GSH oxidation and quantification

The GO-mediated glutathione (GSH) oxidation was monitored according to a modified method (Pasquini et al. 2013).

Briefly, bicarbonate buffer (50 mM, pH = 8.6) was applied to prepare GSH solution (0.8 mM) and GO dispersions (10, 20, 40, 80, 160 mg/L). Each GO dispersion was mixed with the same volume of GSH solution, and then the mixtures were placed in a shaker at 150 rpm for 2 h. After incubation, Ellman’s reagents were added to yield a yellow product (Ellman 1959). The mixtures were filtered through 0.45-µm nylon membranes to remove GO, and the absorbance at 412 nm was measured to determine the amount of non-oxidized GSH. GSH solution without GO was used as control. All experiments were repeated three times, and the loss of GSH was calculated by the following formula:

$$\text{Loss of GSH (\%)} = (A_c - A_e) / A_c \quad (1)$$

where A<sub>c</sub> and A<sub>e</sub> are absorbance of control and experimental samples at 412 nm, respectively.

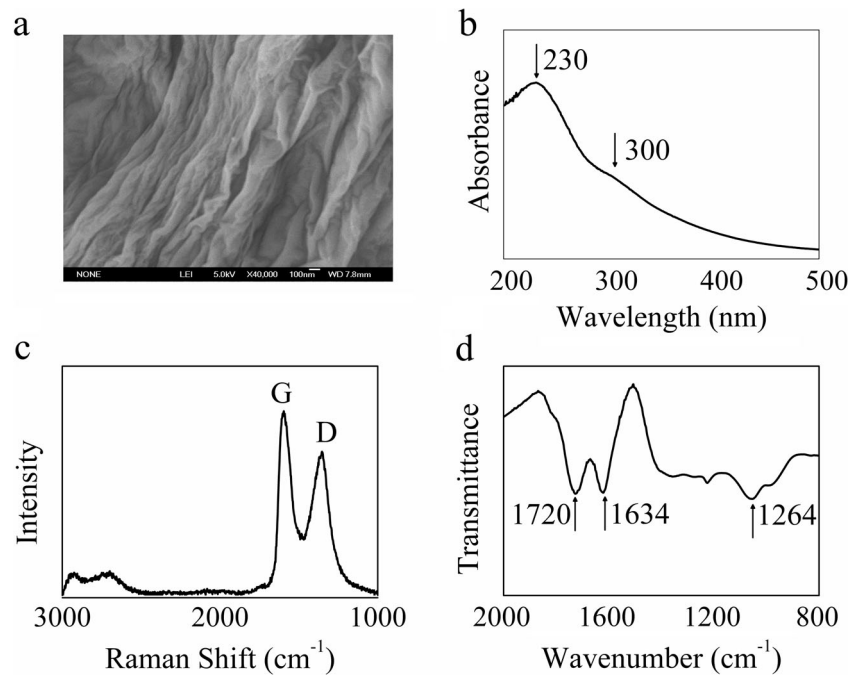
## Results and discussion

### Characterization of GO

In this study, SEM was carried out to evaluate the morphology and structure of the prepared GO. As shown in Fig. 1a, GO was composed of multilayer structure, which is similar with that reported in other studies (Zhao et al. 2011). In addition, carbon and oxygen were the main component elements of GO, and the oxygen concentration was 28.83% atomic percent (Atomic%) (Table S1), which was according with the typical GO produced with Hummers methods (Hummers Jr and Offeman 1958). In UV-Vis spectra, a main absorbance peak was detected at ~ 230 nm, which was attributed to the π-π\* transitions of C=C bond. Besides, a shoulder appeared at ~ 300 nm due to the n-π\* transitions of C=O. The two signals were commonly considered as the typical characteristic absorption peaks of GO (Kumar et al. 2014, Zhang et al. 2010).

The chemical properties of GO were also confirmed by Raman and FTIR spectroscopy. In the Raman spectrum (Fig. 1c), the G band at ~ 1580 cm<sup>-1</sup> is associated with the bond stretching of sp<sup>2</sup> carbon pairs in a graphitic 2D hexagonal lattice (Zhao et al. 2011). The D band at ~ 1350 cm<sup>-1</sup> was attributed to the stretching vibrations of sp<sup>3</sup> carbon atoms, indicating the defects and disorder of GO (Sun et al. 2015). A weak and broad 2D peak was also observed at ~ 2700 cm<sup>-1</sup>, which was correlated with the number of graphene layers (Eda and Chhowalla 2010). For FTIR analysis, the characteristic signals of GO were observed and compared to the previous research (Chen et al. 2013): the signals at ~ 1720 and ~ 1220 cm<sup>-1</sup> were attributed to the stretching vibration of C=O and C–O bond, indicating the presence of oxygen-containing functional groups in graphene oxide. In addition,

**Fig. 1** Characterization of graphene oxide. SEM image (a). UV-Vis spectra (b). Raman spectrum (c). FTIR spectrum (d)



the peak at  $\sim 1620\text{ cm}^{-1}$  was related to the skeletal vibration of C=C from unoxidized  $\text{sp}^2$  CC bonds (Marcano et al. 2010).

### Influence of GO on biofilm formation

*E. coli* and *B. subtilis* were used as the model Gram-negative bacteria and Gram-positive bacteria to evaluate antibacterial activity of GO. Both bacteria were incubated with different concentration of GO in LB medium for 24 h. As shown in Fig. S1, GO could inhibit the cell growth, and the inhibition was enhanced with the increasing GO concentration. The cell viability under the short-term exposure to GO was also measured and shown in Fig. S2. About 70% of *E. coli* and 80% of *B. subtilis* survived after treatment with 10 mg/L GO. Similar to the results of growth profiles, GO at high concentration exhibited much stronger cytotoxicity, and the cell inactivation percentage of *E. coli* and *B. subtilis* with 160 mg/L GO was up to about 90 and 70%, respectively. Moreover, the fluorescence images after live/dead cell staining (Fig. S4) showed that little dead cells were detected in the control groups without GO addition. Lots of dead cells were observed at low GO concentration, and the amount of dead cells increased with the increasing GO concentration. These results were consistent with those in viability assay. Therefore, GO exhibits excellent antibacterial activity, which is in agreement with previous studies (Liu et al. 2011).

In aquatic ecosystem, most bacteria (more than 99%) attach to different surfaces and exist as complex microbial structures, namely, biofilms (Radzig et al. 2013, Rodrigues and Elimelech 2010). When GO is discharged into aquatic ecosystem, it could be adsorbed on the

surface of bacteria and contribute to the formation of biofilm. Therefore, it is necessary and meaningful to evaluate the impacts of GO on biofilm formation. In this study, LB media and minimal M63 supplemented with 0.2% (w/v) glucose were applied to simulate the eutrophic and oligotrophic conditions in natural environment, respectively. The biofilm formation of *E. coli* and *B. subtilis* was evaluated after 48 h of exposure to GO at different dosage (Fig. 2). In the eutrophic environment, the biofilm formation of *E. coli* was obviously enhanced in the presence of GO at 10 mg/L ( $P < 0.05$ ). When GO concentration increased to 20 and 40 mg/L, the *E. coli* biofilm biomass were similar to those without GO addition. However, the formation of biofilm was obviously inhibited with higher-concentration GO addition at 80 and 160 mg/L ( $P < 0.05$ ). Compared to the control without GO addition, the biofilm formation of *B. subtilis* was promoted with 10 mg/L GO, and biofilm biomass decreased with the increasing GO content. With higher GO concentration (160 mg/L), much less biofilm was detected ( $P < 0.001$ ), indicating that biofilm formation was obviously inhibited under high GO stress. Besides, Gram-positive *B. subtilis* exhibited higher resistance as compared to the Gram-negative *E. coli*, which was in accordance with cell viability assay (Fig. S2). The differential toxicity of GO on *E. coli* and *B. subtilis* might be attributed to the structural difference in cell wall of Gram-positive and Gram-negative bacteria (Krishnamoorthy et al. 2012). Gram-positive bacteria have a much thicker peptidoglycan layer (about 20–80 nm) than that of Gram-negative species (7–8 nm) (Fayaz et al. 2010). In the oligotrophic environment, the



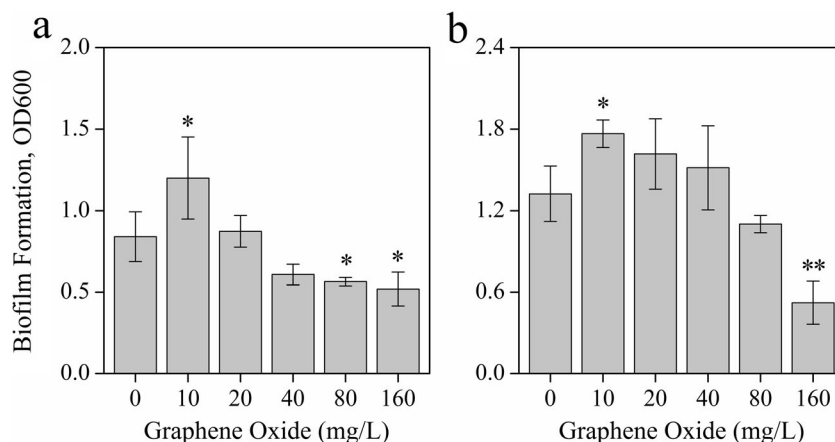


**Fig. 2** Effects of graphene oxide on biofilm formation of *E. coli* (a) and *B. subtilis* (b). Overnight bacteria cultures were inoculated at 1% in 24-well plates containing 2 mL LB medium with different concentrations of graphene oxide. The wells without graphene oxide were set as control groups. All the plates were incubated at 90 rpm for 48 h. The cultivation temperature was 37 °C for *E. coli* and 30 °C for *B. subtilis*. The biofilm

formation was detected with crystal violet staining, and the absorbance was measured at 600 nm. All experiments were conducted in triplicate, and the error bars represent the standard deviations calculated for each independent experiment. The differences of data comparing to control groups were determined with *t* tests with  $P < 0.05$  (\*) as a significant difference and  $P < 0.001$  (\*\*) as a highly significant difference

influences of GO on the biofilm formation of *E. coli* and *B. subtilis* were similar but not quite obvious (Fig. S3), which might be due to the restricted cell growth and activity in the oligotrophic environment. It is interesting that GO may enhance the biofilm product at lower concentrations and inhibit biofilm formation at higher concentrations, whereas it was also found that GO could inhibit and even kill suspended bacteria (Figs. S1, S2, and S4). In suspension, most cells were in contact with GO directly and were inhibited under GO exposure. However, GO could directly interact with part of cells during biofilm formation, which may protect other cells from being in contact with GO (Rodrigues and Elimelech 2010). Hence, the cells in direct contact with GO might play an important role in the formation of biofilm.

**The role of dead cells during biofilm formation**

Membrane stress, induced by extremely sharp edges of nano-sheets, was one of the main antibacterial mechanisms of GO (Liu et al. 2011). Previous studies have shown that GO could damage the cell membrane with the extremely sharp edges through direct contact with bacteria, leading to the efflux of cytoplasmic materials, such as proteins and RNA (Akhavan and Ghaderi 2010, Kang et al. 2008). The cell not in contact with GO might utilize the released cytoplasmic materials as nutrients for growth and thus enhance the formation of biofilm (Rodrigues and Elimelech 2010). To prove this hypothesis, we evaluated the biofilm formation in the presence of dead cells at different dosages. As shown in Fig. 3, more biofilm can be detected in the presence of higher-concentration dead cells.

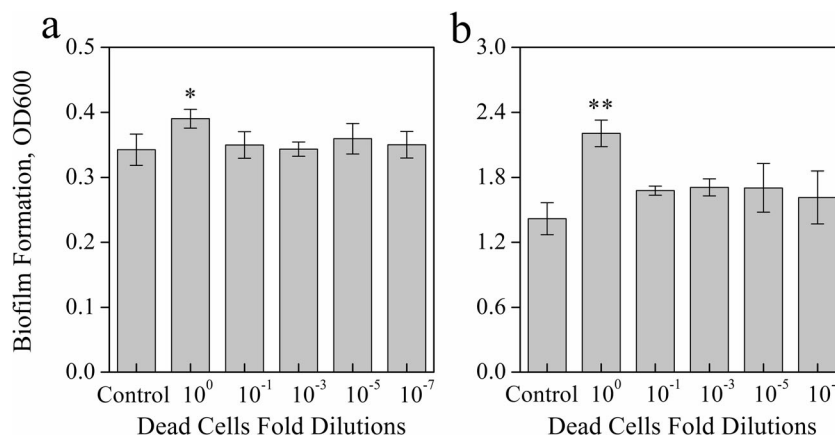


**Fig. 3** Biofilm formation of *E. coli* (a) and *B. subtilis* (b) in the presence of different dilutions of dead cells. Overnight bacteria cultures were inoculated in 24-well plates containing 2 mL M63 medium with different dilutions of dead cells. The wells without dead cells addition were set as control groups. All experiments were repeated four times, and

the error bars represent the standard deviations calculated for each independent experiment. The differences of data comparing to control groups were determined with *t*-tests with  $P < 0.05$  (\*) as a significant difference and  $P < 0.001$  (\*\*) as a highly significant difference

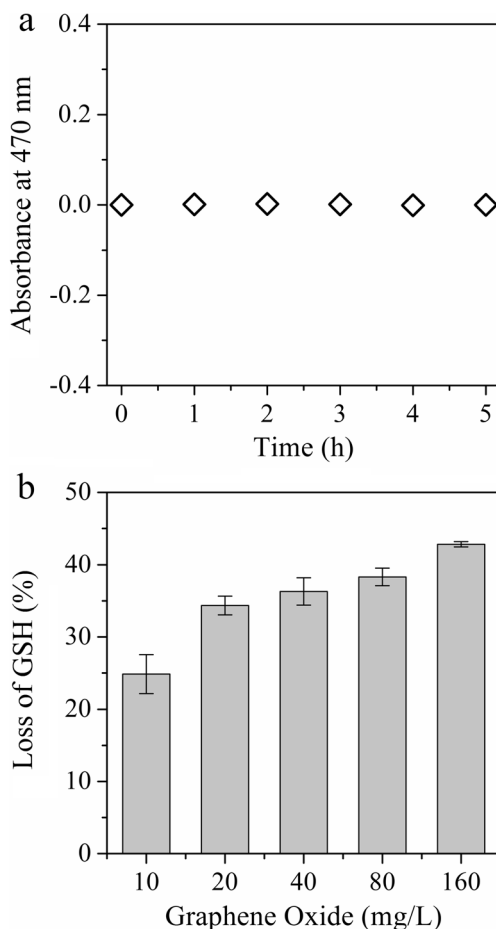


**Fig. 4** Oxidative stress mediated by graphene oxide. **a** Production of  $O_2^-$ . **b** Oxidation of GSH. The yields of  $O_2^-$  were detected using the method by the reduction of XTT. The absorbance at 470 nm was measured to detect XTT-formazan. The content of GSH was detected using Ellman's reagents, and the absorbance at 412 nm was measured to determine the amount of non-oxidized GSH. All experiments were conducted at least in triplicate, and the error bars represent the standard deviations calculated for each independent experiment. The difference between the loss of GSH of different graphene oxide concentrations was verified as highly significant by one-way ANOVA analysis with  $P < 0.001$

For *E. coli*, biofilm formation without dead cell addition was quantified as  $0.34 \pm 0.02$  (OD600) and was regarded as the control. The biofilm biomass increased to  $0.39 \pm 0.01$  when dilution of dead cells was  $10^0$ . Compared with the control at  $1.42 \pm 0.15$ , the biofilm formation of *B. subtilis* was obviously improved to  $2.21 \pm 0.12$  in the presence of dead cells without dilution. Both increases were verified as significant for *E. coli* and highly significant for *B. subtilis* through a significant analysis, suggesting that the addition of dead cells could promote the formation of biofilm. These results indicated that certain amount of dead cells could be utilized as nutrients and enhance the formation of biofilm, which were consistent with other studies (Rodrigues and Elimelech 2010).

In addition, direct GO-bacteria contact is necessary to induce membrane stress, leading to physical damages on cell membranes (Vecitis et al. 2010). In bacterial suspensions, cells

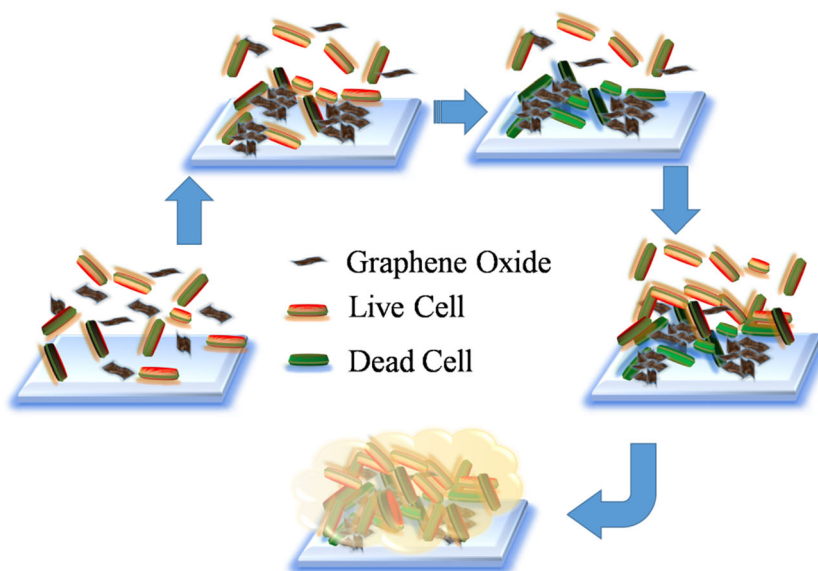
and GO were well dispersed and in contact with each other directly, resulting in growth inhibition or death of bacteria. During the formation of biofilm, cells and GO existed as aggregates or precipitates. When exposed to low concentrations of GO, the cells in direct contact with GO can form a protective barrier to prevent other cells from contacting with GO, resulting in the normal biofilm formation of the cells not in contact with GO. Moreover, dead cells could provide nutrients for live cells to further promote the cell growth. When GO concentrations were high (80–160 mg/L), most bacteria were inactivated (Fig. S2), leading to less biofilm formation. These could explain that biofilm formation was enhanced with low GO concentrations and inhibited in the presence of high-concentration GO.

### Oxidative stress mediated by GO

Besides membrane stress mediated by direct contact, oxidative stress is also considered as one of the main antibacterial mechanisms of carbon nanomaterials (Lyon et al. 2008). In general, oxidative stress against cells arises by two paths: reactive oxygen species (ROS)-mediated oxidative stress and ROS-independent oxidative stress (Liu et al. 2011). The former is attributed to the generation of elevated ROS levels by carbon nanomaterials while the latter is induced by ROS-independent oxidative stress, which could disturb or oxidize a vital cellular structure or component to disrupt the routine cellular function (Pasquini et al. 2013). Based upon the similar structural and physiochemical properties with other carbon nanomaterials, GO might induce ROS-independent oxidative stress, resulting in the inactivation of cells.

Superoxide anion ( $O_2^-$ ), the main ROS mediated by carbon nanomaterials, was first evaluated using XTT as a colorimetric probe (Hsieh and Jafvert 2015). XTT can be reduced by superoxide anion to generate XTT-formazan, which is a soluble yellow compound with characteristic absorption at 470 nm (Sutherland and Learmonth 1997). As shown in Fig. 4a, no noticeable absorption was detected at 470 nm during the 5-h reaction, implying that no  $O_2^-$  is generated. Therefore, ROS-mediated oxidative stress might play a minor role in the antibacterial activity of GO. In addition, the ROS-independent oxidative stress was investigated with GSH as an indicator. GSH, an antioxidant in bacteria, could diminish oxidative damages to cells induced by oxidative stress (Pompella et al. 2003). Hence, the loss of GSH is usually applied to quantify the ROS-independent oxidative stress towards bacterial cells. About 25% of GSH was oxidized in the presence of 10 mg/L GO, and the loss of oxidation increased with the increasing GO concentrations (Fig. 4b). These results suggested that GO could induce the ROS-independent oxidative stress, which contributed to the antibacterial activity of GO.

**Fig. 5** Proposed mechanism for the effects of graphene oxide on biofilm formation



**Mechanism of GO on biofilm formation**

In general, a biofilm forms through several stages, including the development, maturation, and disassembly of the bacterial community (Vlamakis et al. 2013). In the initial phase, dissociative cells would aggregate or attach onto the surface of solid, and then further develop to form mature biofilm. According to the results above mentioned, we proposed the possible mechanism of GO on biofilm formation (Fig. 5). When releasing into aquatic environment, GO would first disperse in solution and encounter with bacteria. Due to the ecological adaption of individual member, planktonic cells aggregate together to generate biofilm via cellular plasticity (Li et al. 2017). Exposed to GO, bacteria cells would be inhibited or killed via the membrane stress and oxidative stress induced by GO, which results in dead cells. When the amount of GO is low, only part of cells make contact with GO directly and deposit with the aggregation of GO, which form a protective barrier to prevent the other cells from contacting with GO. Meanwhile, the dead cells also promote the growth of live cells as nutriment. Then, the live cells chain and bundle with each other to produce more mature biofilms. However, nearly all bacteria were inactivated under high GO stress, leading to negligible live cells to form biofilm at the initiation stage. Thus, the biofilm formation was inhibited in the presence of high-concentration GO.

**Conclusions**

In this study, we evaluated the biofilm formation of both Gram-negative bacteria and Gram-positive bacteria in the presence of GO. GO exhibited a high antibacterial activity via membrane stress and ROS-independent oxidative stress. However, biofilm

formation was enhanced with the addition of low-concentration GO and inhibited when exposed to high-concentration GO. This may be due to the fact that only a part of living cells was killed by a limited concentration of GO, and the dead cells could serve as a protection barrier and nutrient to the rest for biofilm formation, whereas nearly all cells were inactivated under overwhelming GO stress, leading to negligible biofilm formation in the high-concentration GO environment.

**Funding information** The research was supported by the National Natural Science Foundation of China (21676161, 21476130 and 51208283).

**References**

Akhavan O, Ghaderi E (2010) Toxicity of graphene and graphene oxide nanowalls against bacteria. *ACS Nano* 4:5731–5736

Bar-Zeev E, Passow U, Romero-Vargas Castrillón S, Elimelech M (2015) Transparent exopolymer particles: from aquatic environments and engineered systems to membrane biofouling. *Environ Sci Technol* 49:691–707

Blaustein RA, Shelton DR, Van Kessel JAS, Kams JS, Stocker MD, Pachepsky YA (2015) Irrigation waters and pipe-based biofilms as sources for antibiotic-resistant bacteria. *Environ Monit Assess* 188: 56

Chen J, Yao BW, Li C, Shi GQ (2013) An improved hummers method for eco-friendly synthesis of graphene oxide. *Carbon* 64:225–229

Chowdhury I, Duch MC, Mansukhani ND, Hersam MC, Bouchard D (2013) Colloidal properties and stability of graphene oxide nanomaterials in the aquatic environment. *Environ Sci Technol* 47: 6288–6296

Costerton JW, Stewart PS, Greenberg EP (1999) Bacterial biofilms: a common cause of persistent infections. *Science* 284:1318–1322

Ding LH, Stilwell J, Zhang TT, Elboudwarej O, Jiang HJ, Selegue JP, Cooke PA, Gray JW, Chen FF (2005) Molecular characterization of the cytotoxic mechanism of multiwall carbon nanotubes and nanoions on human skin fibroblast. *Nano Lett* 5:2448–2464

- Eda G, Chhowalla M (2010) Chemically derived graphene oxide: towards large-area thin-film electronics and optoelectronics. *Adv Mater* 22:2392–2415
- Ellman GL (1959) Tissue sulfhydryl groups. *Arch Biochem Biophys* 82: 70–77
- Fayaz AM, Balaji K, Girilal M, Yadav R, Kalaichelvan PT, Venketesan R (2010) Biogenic synthesis of silver nanoparticles and their synergistic effect with antibiotics: a study against gram-positive and gram-negative bacteria. *Nanomedicine* 6:103–109
- Greendyke R, Byrd TF (2008) Differential antibiotic susceptibility of *Mycobacterium abscessus* variants in biofilms and macrophages compared to that of planktonic bacteria. *Antimicrob Agents Chemother* 52:2019–2026
- Gurunathan S, Han JW, Dayem AA, Eppakayala V, Kim J-H (2012) Oxidative stress-mediated antibacterial activity of graphene oxide and reduced graphene oxide in *Pseudomonas aeruginosa*. *Int J Nanomedicine* 7:5901
- Hsieh H-S, Jafvert CT (2015) Reactive oxygen species generation and dispersant-dependent electron transfer through single-walled carbon nanotubes in water. *Carbon* 89:361–371
- Hummers Jr WS, Offeman RE (1958) Preparation of graphitic oxide. *J Am Chem Soc* 80:1339–1339
- Jackson DW, Suzuki K, Oakford L, Simecka JW, Hart ME, Romeo T (2002) Biofilm formation and dispersal under the influence of the global regulator CsrA of *Escherichia coli*. *J Bacteriol* 184:290–301
- Jewell KS, Falás P, Wick A, Joss A, Temes TA (2016) Transformation of diclofenac in hybrid biofilm-activated sludge processes. *Water Res* 105:559–567
- Kang S, Herzberg M, Rodrigues DF, Elimelech M (2008) Antibacterial effects of carbon nanotubes: size does matter. *Langmuir* 24:6409–6413
- Krishnamoorthy K, Veerapandian M, Zhang LH, Yun K, Kim SJ (2012) Antibacterial efficiency of graphene nanosheets against pathogenic bacteria via lipid peroxidation. *J Phys Chem C* 116:17280–17287
- Kumar PV, Bardhan NM, Tongay S, JQ W, Belcher AM, Grossman JC (2014) Scalable enhancement of graphene oxide properties by thermally driven phase transformation. *Nature Chem* 6:151–158
- Li Q, Xia PF, Tao ZY, Wang SG (2017) Modeling biofilms in water systems with new variables: a review. *Water* 9:462
- Liu SB, Zeng TH, Hofmann M, Burcombe E, Wei J, Jiang RR, Kong J, Chen Y (2011) Antibacterial activity of graphite, graphite oxide, graphene oxide, and reduced graphene oxide: membrane and oxidative stress. *ACS Nano* 5:6971–6980
- Liu S, Gunawan C, Barraud N, Rice SA, Harry EJ, Amal R (2016) Understanding, monitoring, and controlling biofilm growth in drinking water distribution systems. *Environ Sci Technol* 50:8954–8976
- Lv T, Carvalho PN, Zhang L, Zhang Y, Button M, Arias CA, Weber KP, Brix H (2017) Functionality of microbial communities in constructed wetlands used for pesticide remediation: influence of system design and sampling strategy. *Water Res* 110:241–251
- Lyon DY, Brunet L, Hinkal GW, Wiesner MR, Alvarez PJ (2008) Antibacterial activity of fullerene water suspensions (nC60) is not due to ROS-mediated damage. *Nano Lett* 8:1539–1543
- Manna SK, Sarkar S, Barr J, Wise K, Barrera EV, Jejelowo O, Rice-Ficht AC, Ramesh GT (2005) Single-walled carbon nanotube induces oxidative stress and activates nuclear transcription factor- $\kappa$ B in human keratinocytes. *Nano Lett* 5:1676–1684
- Marcano DC, Kosynkin DV, Berlin JM, Sinitskii A, Sun Z, Slesarev A, Alemany LB, Lu W, Tour JM (2010) Improved synthesis of graphene oxide. *ACS Nano* 4:4806–4814
- Musico YLF, Santos CM, Dalida MLP, Rodrigues DF (2014) Surface modification of membrane filters using graphene and graphene oxide-based nanomaterials for bacterial inactivation and removal. *ACS Sustain Chem Eng* 2:1559–1565
- Pasquini LM, Sekol RC, Taylor AD, Pfefferle LD, Zimmerman JB (2013) Realizing comparable oxidative and cytotoxic potential of single- and multiwalled carbon nanotubes through annealing. *Environ Sci Technol* 47:8775–8783
- Perreault F, De Faria AF, Nejati S, Elimelech M (2015) Antimicrobial properties of graphene oxide nanosheets: why size matters. *ACS Nano* 9:7226–7236
- Pompella A, Visvikis A, Paolicchi A, De Tata V, Casini AF (2003) The changing faces of glutathione, a cellular protagonist. *Biochem Pharmacol* 66:1499–1503
- Radzig MA, Nadtochenko VA, Koksharova OA, Kiwi J, Lipasova VA, Khmel IA (2013) Antibacterial effects of silver nanoparticles on gram-negative bacteria: influence on the growth and biofilms formation, mechanisms of action. *Colloids Surf B: Biointerfaces* 102: 300–306
- Reid T, VanMensel D, Droppo IG, Weisener CG (2016) The symbiotic relationship of sediment and biofilm dynamics at the sediment water interface of oil sands industrial tailings ponds. *Water Res* 100:337–347
- Rodrigues DF, Elimelech M (2010) Toxic effects of single-walled carbon nanotubes in the development of *E. coli* biofilm. *Environ Sci Technol* 44:4583–4589
- Rudrappa T, Biedrzycki ML, Bais HP (2008) Causes and consequences of plant-associated biofilms. *FEMS Microbiol Ecol* 64:153–166
- Schembri MA, Kjærsgaard K, Klemm P (2003) Global gene expression in *Escherichia coli* biofilms. *Mol Microbiol* 48:253–267
- Sotirelis NP, Chrysikopoulos CV (2015) Interaction between graphene oxide nanoparticles and quartz sand. *Environ Sci Technol* 49: 13413–13421
- Sun XF, Qin J, Xia PF, Guo BB, Yang CM, Song C, Wang SG (2015) Graphene oxide–silver nanoparticle membrane for biofouling control and water purification. *Chem Eng J* 281:53–59
- Sutherland MW, Learmonth BA (1997) The tetrazolium dyes MTS and XTT provide new quantitative assays for superoxide and superoxide dismutase. *Free Radic Res* 27:283–289
- Vecitis CD, Zodrow KR, Kang S, Elimelech M (2010) Electronic-structure-dependent bacterial cytotoxicity of single-walled carbon nanotubes. *ACS Nano* 4:5471–5479
- Vlamakis H, Chai YR, Beaugard P, Losick R, Kolter R (2013) Sticking together: building a biofilm the *Bacillus subtilis* way. *Nature Reviews Microbiology* 11:157–168
- Xia TJ, Fortner JD, Zhu DQ, Qi ZC, Chen W (2015) Transport of sulfide-reduced graphene oxide in saturated quartz sand: cation-dependent retention mechanisms. *Environ Sci Technol* 49:11468–11475
- Zhang JL, Yang HJ, Shen GX, Cheng P, Zhang JY, Guo SW (2010) Reduction of graphene oxide via L-ascorbic acid. *Chem Commun* 46:1112–1114
- Zhao GX, Li JX, Ren XM, Chen CL, Wang XK (2011) Few-layered graphene oxide nanosheets as superior sorbents for heavy metal ion pollution management. *Environ Sci Technol* 45:10454–10462